INORGANIC CHEMISTRY FRONTIERS

RESEARCH ARTICLE

View Article Online
View Journal | View Issue

Cite this: *Inorg. Chem. Front.*, 2025, **12**, 3595

$CdF(C_6H_4NO_2)(H_2O)$: a UV nonlinear optical material with unprecedented SHG and birefringence *via* π-conjugated rings and a unique "Warren truss structure"†

Jie Gou,‡[a,b] Yaolong Zhu,‡[a] Xin Su,[b] Can Yang,[a] YunJie Wang,[b] Qingwen Zhu,[a] Yi Xiong[a] and Qi Wu*[a]

Received 20th February 2025,
Accepted 10th March 2025

DOI: 10.1039/d5qi00517e

rsc.li/frontiers-inorganic

We report the design and synthesis of a novel ultraviolet (UV) nonlinear optical (NLO) material, $CdF(C_6H_4NO_2)(H_2O)$, featuring a unique "Warren truss structure". This material exhibits a two-dimensional (2D) layered architecture structure composed of highly polarized $[CdNO_2F_3]$ octahedra and π-conjugated organic rings $(C_6H_4NO_2)^-$. Notably, $CdF(C_6H_4NO_2)(H_2O)$ demonstrates exceptional second-harmonic generation (SHG) response, with an intensity 3.2 times that of KH_2PO_4 (KDP), and a large birefringence of 0.26@546 nm, which is highly unusual for UV fluorides with a bandgap of >4.2 eV. Theoretical calculations and structural analysis reveal that the introduction of $(C_6H_4NO_2)^-$ into CdF_2 induces significant structural distortion and polarization, leading to the formation of a non-centrosymmetric "Warren truss structure". This structure aligns $[CdNO_2F_3]$ octahedra and organic rings in a highly ordered manner, which is crucial for the enhanced SHG and large birefringence. Our findings provide a new strategy for designing high-performance UV NLO materials by leveraging organic–inorganic hybrid structures.

Introduction

The rapid advancement of quantum technology (QT) is revolutionizing the capabilities of communication multiplexing and high-dimensional quantum information processing, with significant implications for spin–orbit angular momentum photonics. In this context, materials with strong second-harmonic generation (SHG) effects and high birefringence are urgently needed to enhance quantum optical techniques, particularly for efficient frequency doubling and precise manipulation of photons carrying orbital angular momentum (OAM).[1–3] However, the development of such materials is hindered by the contrasting microstructural requirements for SHG and birefringence, making it challenging to meet both criteria simultaneously. This is especially true in the ultraviolet (UV) band, where materials with a bandgap of >4.2 eV are required, but few exhibit both strong SHG and large birefringence.

Fluorine, often referred to as the "star element" in nonlinear optical (NLO) materials, is known for its highest electronegativity, which significantly influences crystal structure regulation and optical bandgap enhancement.[4] Its incorporation optimizes birefringence and reduces refractive index dispersion, thereby enabling shorter phase-matching wavelengths.[5] Over the past decade, more than 200 fluorides and their derivatives have been reported, playing a crucial role in optoelectronic applications. However, despite their potential, these materials often fail to combine a large bandgap (>4.2 eV), strong SHG (>3 times KDP), and high birefringence (>0.2).[6–23] Pure metal fluorides, while gaining attention as UV NLO materials, are similarly limited by weak SHG and small birefringence.[24,25] These limitations have significantly restricted the application of fluorides and their derivatives in quantum optical technologies.

Recently, planar conjugated organic rings have garnered significant attention due to their remarkable enhancement of SHG and birefringence. For example, organic groups such as $(H_2C_6N_9)^-$, $(C_7H_4NO_4)^+$, $(C_3N_6H_7)^+$, and $(C_3N_2H_5)^+$ exhibit high optical activity and have been used to construct large birefringent crystals.[26–29] Similarly, groups like $(C_3N_3O_3)^{3-}$, $(C_5H_6NO)^+$, $(HC_3N_3S_3)$, and $(H_2C_6N_7O_3)^-$ have been identified as excellent NLO active units.[30–33] These findings suggest that

[a]*State Key Laboratory of New Textile Materials and Advanced Processing, Wuhan Textile University, Wuhan 430200, People's Republic of China. E-mail: wuqi2011@whu.edu.cn*

[b]*Xinjiang Laboratory of Phase Transitions and Microstructures in Condensed Matter Physics, College of Physical Science and Technology, Yili-Normal University, Yi Ning, 835000, China*

†Electronic supplementary information (ESI) available. CCDC 2419363. For ESI and crystallographic data in CIF or other electronic format see DOI: https://doi.org/10.1039/d5qi00517e

‡These authors contributed equally to this work.

incorporating metal fluorides into organic rings could be an effective strategy to enhance SHG and birefringence. However, this approach remains largely unexplored, particularly for UV-transmitting materials with strong SHG and birefringence.

Metal fluoride CdF_2, despite its potential as a UV NLO material, lacks SHG due to its centrosymmetric structure, and its calculated birefringence (0.00002@546.1 nm) is negligible. Here, we report the synthesis of a novel metal–organic complex, $CdF(C_6H_4NO_2)(H_2O)$, by introducing the π-conjugated organic ring $(C_6H_4NO_2)^-$ into CdF_2. This substitution not only breaks the centrosymmetry but also induces significant polarization anisotropy and second-order hyperpolarizability. Compared to the centrosymmetric CdF_2 (SHG = 0, negligible birefringence of 0.00002@546 nm), the resulting compound, $CdF(C_6H_4NO_2)(H_2O)$, exhibits remarkably enhanced SHG (3.2×KDP) and birefringence (0.26@546 nm), while maintaining UV transmittance (band gap = 4.41 eV). This material represents a rare example of UV metal fluoride combining strong SHG and high birefringence. Our comprehensive study, including design, synthesis, structural analysis, properties, and theoretical calculations, reveals how the π-conjugated organic ring $(C_6H_4NO_2)^-$ constructs a "Warren truss structure" in semi-organic metal fluorides. This unique structure aligns highly polarized $[CdNO_2F_3]$ octahedra, leading to the observed strong SHG and large birefringence. Our findings not only advance the understanding of SHG and birefringence enhancement in metal fluorides but also highlight the potential applications of $CdF(C_6H_4NO_2)(H_2O)$ in quantum optical technologies.

Results and discussion

The design idea of $CdF(C_6H_4NO_2)(H_2O)$ is mainly based on the use of $(C_6H_4NO_2)^-$ with a planar π-conjugated organic ring to replace F^- in the simple metal fluoride CdF_2. $CdF(C_6H_4NO_2)(H_2O)$ is obtained using a hydrothermal method as detailed in the ESI.† As shown in Scheme 1, during the reaction process, since CdF_2 is a strong base and weak acid salt, the entire reaction system is acidic. Initially, the raw material methyl nicotinate (S1) hydrolyzes to form nicotinic acid (S2) and methanol. Then, S2 reacts with F^- to produce S3 and the weak acid HF, thereby exposing two coordination active sites of N and O. Subsequently, S3, F^-, and H_2O coordinate with Cd^{2+} to form $CdF(C_6H_4NO_2)(H_2O)$.

Fig. 1a and b illustrate the structural transformation from the precursor CdF_2 to the product $CdF(C_6H_4NO_2)(H_2O)$. The introduction of the organic ring $(C_6H_4NO_2)^-$ disrupts the interconnected $[(Cd_2F_2)^{2+}]_\infty$ chains, forming a unique structure resembling a "Warren truss bridge" within the two-dimensional plane. The rigid organic ring $(C_6H_4NO_2)^-$ acts as the "diagonal" of the bridge, connecting to Cd through coordination atoms at both ends, thereby forming a stable triangular structure that supports the "top/bottom chord" of the bridge, namely the $[(Cd_2F_2)^{2+}]_\infty$ chains, aligning them in a completely parallel and consistent arrangement. The addition of $(C_6H_4NO_2)^-$ transforms the cubic $[CdF_8]$ in CdF_2 into a distorted octahedron $[CdNO_2F_3]$, resulting in structural symmetry breaking from a centrosymmetric to a non-centrosymmetric structure.

$CdF(C_6H_4NO_2)(H_2O)$ crystallizes in the polar space group $P2_1$ with unit cell parameters of a = 9.2128 Å, b = 4.2589 Å, c = 10.740 Å, $\alpha = \gamma = 90°$, β = 114.506(4)°, and V = 383.44(10) Å^3 (detailed information is provided in Table S1†). Its CCDC number is 2419363.† The metal Cd is coordinated with one N and one O from two organic rings $(C_6H_4NO_2)^-$, one water molecule, and three F ions, forming a distorted $[CdNO_2F_3]$ octahedron. The bond lengths of Cd–N, Cd–O, and Cd–F are 2.302 Å, 2.216–2.303 Å, and 2.195–2.311 Å, respectively, which are consistent with previously reported literature (Fig. 2a).[34] As shown in Fig. 2b, the $[CdNO_2F_3]$ octahedra with two orientations are alternately arranged along the b-axis, forming a zigzag one-dimensional chain. These chains are interconnected by the organic rings $(C_6H_4NO_2)^-$ (the distance between two chains is 9.2128 Å, and the angle of the organic ring is 59.2°, as shown in Fig. S1†), creating a unique structure resembling a "Warren truss bridge". They extend infinitely along the ab plane to form a two-dimensional layer. Subsequently, these two-dimensional layers are closely stacked along the c-axis in the same orientation, ultimately forming the unique spatial structure of $CdF(C_6H_4NO_2)(H_2O)$ (Fig. 2c and d).

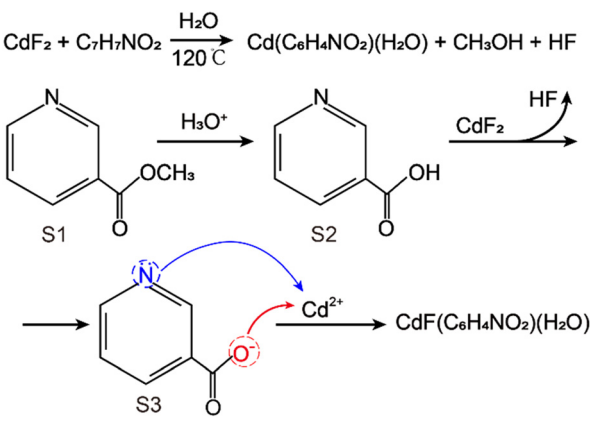

Scheme 1 Synthesis and mechanism of $CdF(C_6H_4NO_2)(H_2O)$.

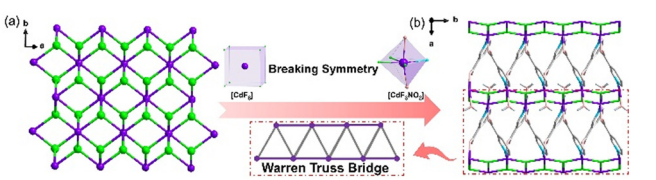

Fig. 1 Transition from a centrally symmetrical CdF_2 structure (a) to a NCS structure of $CdF(C_6H_4NO_2)(H_2O)$ (b). The upper part of the red arrow indicates the evolution of the cube $[CdF_8]$ to the twisted octahedron $[CdNO_2F_3]$. Below the red arrow, a comparison of the $CdF(C_6H_4NO_2)(H_2O)$ structure with the Warren truss bridge is shown.

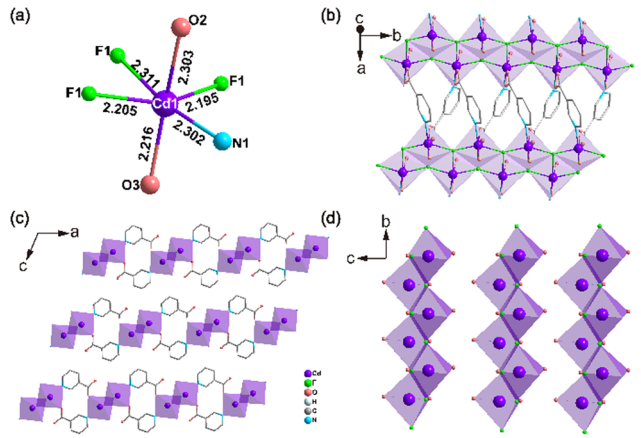

Fig. 2 (a) The coordination environment of Cd; (b) the two-dimensional layered structure of $CdF(C_6H_4NO_2)(H_2O)$ in space; (c) the structure of $CdF(C_6H_4NO_2)(H_2O)$ in the *ac* plane; (d) the structure of $CdF(C_6H_4NO_2)(H_2O)$ in the *bc* plane.

XPS spectral analysis of $CdF(C_6H_4NO_2)(H_2O)$ (Fig. 3a, b and S6, S7†) confirms Cd's oxidation state as Cd^{2+} with peaks at 404.65 eV and 412.62 eV in the 402–414 eV binding energy range and F's oxidation state as −1, consistent with the results of BVS calculations (Table S2†) and single-crystal structure resolution. The band gap of $CdF(C_6H_4NO_2)(H_2O)$ is 4.41 eV, measured using the Kubelka–Munk method (Fig. 3c),[35] exceeding the 4.2 eV threshold for UV NLO materials and surpassing reported values for Na_2CeF_6 (3.89 eV),[36] KBi_4F_{13} (4.24 eV),[37] and $K_2SbF_2Cl_3$ (4.01 eV),[38] indicating its UV application potential. IR absorption peaks align with single-crystal test results (Fig. S3†), and thermogravimetric tests show stability up to 150 °C (Fig. S4†).

The Kurtz–Perry method was used to measure[39] the SHG response of $CdF(C_6H_4NO_2)(H_2O)$ under 1064 nm laser irradiation. Its SHG intensity increases with particle size, plateaus at 280–450 μm, and shows phase matching behavior. Within this size range, its SHG intensity is about 3.2×KDP (Fig. 3d and e). Generally, metal fluorides have weak NLO effects due to fluorine's weak deformability. For instance, the SHG responses of KNa_2ZrF_7 (0.35×KDP),[4] $CsNaTaF_7$ (0.20×KDP),[40] $BaMgF_4$ (0.085×KDP),[41] $BaZnF_4$ (0.16×KDP),[42] Na_2SbF_5 (0.17×KDP),[43] and Na_2CeF_6 (2.1×KDP)[36] are all less than 1×KDP. Although Na_2CeF_6 has a rare 2.1×KDP SHG response, its 3.89 eV optical band gap limits its UV band application. Fig. 3f shows the comparison of the optical band gaps and SHG effects of recent metal fluorides (Table S8†), showing that $CdF(C_6H_4NO_2)(H_2O)$'s SHG effect is the strongest among those of recent UV NLO metal fluorides with a band gap of >4.2 eV. Further dipole moment analysis reveals a calculated dipole moment of 6.14 D for $CdF(C_6H_4NO_2)(H_2O)$, aligning with its SHG intensity.

The second harmonic generation (SHG) effect is generally diminished in fluorides with short absorption edges. The origin of the nonlinear optical (NLO) efficiency is predominantly contingent on the asymmetry and arrangement of the polyhedra within the crystal structure. In the compound $CdF(C_6H_4NO_2)(H_2O)$, the severely distorted octahedra $[CdNO_2F_3]$ constitute a one-dimensional sawtooth chain. Subsequently, these chains are interconnected by the organic ring

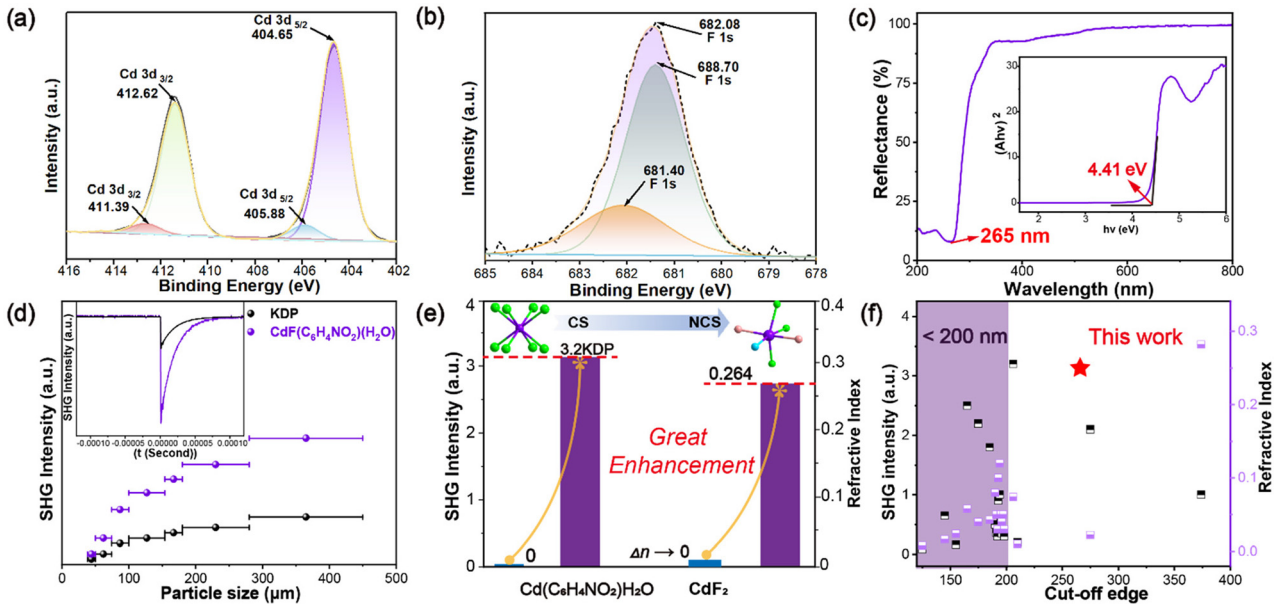

Fig. 3 (a) XPS spectrum of Cd-3d in $CdF(C_6H_4NO_2)(H_2O)$. (b) XPS spectrum of F-1s in $CdF(C_6H_4NO_2)(H_2O)$. (c) UV spectrum of $CdF(C_6H_4NO_2)(H_2O)$. (d) The particle size of $CdF(C_6H_4NO_2)(H_2O)$ and KDP as a function of the SHG response. The inset is a SHG intensity signal plot of $CdF(C_6H_4NO_2)(H_2O)$ with KDP in the particle size range of 280–450 μm. (e) Comparison of SHG response and birefringence performance of $CdF(C_6H_4NO_2)(H_2O)$ and CdF_2. (f) Scatter plots of bandgap, birefringence and SHG intensities of $CdF(C_6H_4NO_2)(H_2O)$ *versus* various fluorides. (Black on the left indicates SHG, purple on the right represents birefringence, and black at the bottom denotes the cut-off edge.)

$(C_6H_4NO_2)^-$, culminating in a distinctive "Warren truss bridge" structure. This unique configuration facilitates the optimal alignment of the $[CdNO_2F_3]$ octahedra and $(C_6H_4NO_2)^-$ within the crystal lattice, which is the pivotal factor enabling the large SHG and high birefringence of $CdF(C_6H_4NO_2)(H_2O)$. These structural analyses offer invaluable insights into the design of NLO materials with enhanced SHG effects, potentially guiding future research endeavors in this domain.

The birefringence of $CdF(C_6H_4NO_2)(H_2O)$ single crystals, measured using a polarizing microscope (Fig. 4a), was found to be 0.253@546.1 nm for a crystal thickness of 7 μm (Fig. 4b–d). This value exceeds those of commercial birefringent crystals such as MgF_2 (0.012@589.3 nm),[44] α-BaB_2O_4 (0.122@532 nm),[45] and $CaCO_3$ (0.172@589 nm)[46] and represents the upper limit of UV pure metal fluorides and semi-organometallic fluorides (Table S8†), except for $(H_2DpA)_2SiF_6$(0.282).[47] $(H_2DpA)_2SiF_6$ has only 1×KDP and a band gap of 2.84 eV, significantly lower than the required 4.2 eV and 3×KDP. The calculated linear optical properties (Fig. 4e) reveal strong anisotropy with refractive indices n_z = 1.764, n_x = 1.745, and n_y = 1.511, yielding birefringence Δn = 0.264@546 nm, agreeing well with the measured value. Additionally, the birefringence of CdF_2 at 546 nm was calculated to be 0.00002 (Fig. 4f), which is nearly 10 000 times lower than that of $CdF(C_6H_4NO_2)(H_2O)$.

First-principles density-functional theory calculations (Fig. S8–S11†) reveal that $CdF(C_6H_4NO_2)(H_2O)$ and CdF_2 have indirect band gaps of 3.507 and 3.743 eV, respectively. The density of states diagram (Fig. S11†) shows that the valence band top is dominated by O-2p orbitals with minor F-2p contributions, while the conduction band bottom is influenced by C-2p, N-2p, and O-2p orbitals. This indicates that the band gap of $CdF(C_6H_4NO_2)(H_2O)$ is primarily determined by the $(C_6H_4NO_2)^-$ unit, with minimal contribution from Cd–F interactions (Fig. 5b).

Quantum chemistry-based frontier orbital calculations on $CdF(C_6H_4NO_2)(H_2O)$ primitives reveal the contributions of $[CdNO_2F_3]$ and $(C_6H_4NO_2)^-$ units. In $CdF(C_6H_4NO_2)(H_2O)$, the HOMO is dominated by F-2p and Cd-4d orbitals, while the LUMO is primarily influenced by the $(C_6H_4NO_2)^-$ unit and Cd and F orbitals within the $[CdNO_2F_3]$ octahedron (Fig. S12 and S13†). These d–p hybridization events facilitate electron movement, under the photoelectric field, enhancing the second-harmonic generation (SHG) effect.

Under Kleinman symmetry constraints,[48] $CdF(C_6H_4NO_2)(H_2O)$ exhibits four independent nonzero SHG coefficients: d_{14} = −0.241 pm V^{-1}, d_{16} = 1.114 pm V^{-1}, d_{22} = 0.747 pm V^{-1}, and d_{23} = −0.439 pm V^{-1}, with d_{16} being the largest and consistent with experimental results. Further investigation through SHG-weighted density maps (Fig. 5a, b and S14, S15†) shows that the occupied states in the virtual electron (VE) and virtual hole

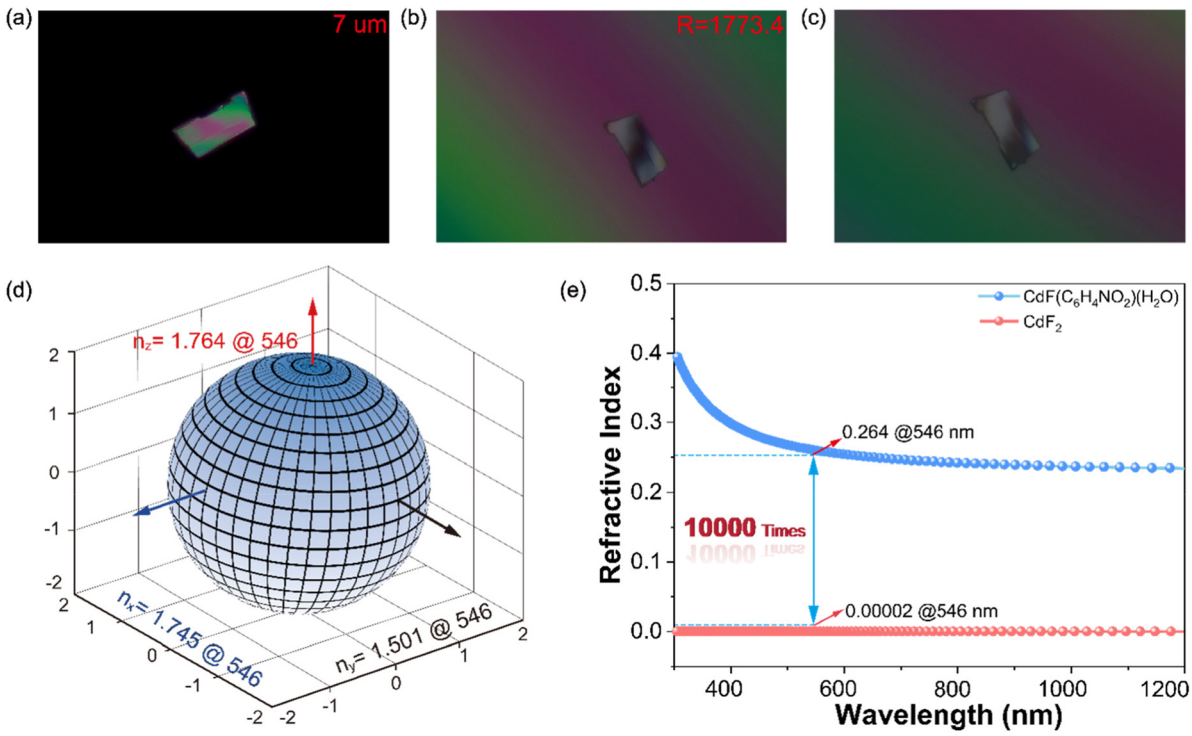

Fig. 4 (a) Thickness of selected wafers measured using the birefringence of $CdF(C_6H_4NO_2)(H_2O)$. (b and c) $CdF(C_6H_4NO_2)(H_2O)$ extinguished under cross-polarized light. (d) Theoretically calculated refractive index of $CdF(C_6H_4NO_2)(H_2O)$. (e) Comparison of birefringence@546 nm between CdF_2 and $CdF(C_6H_4NO_2)(H_2O)$.

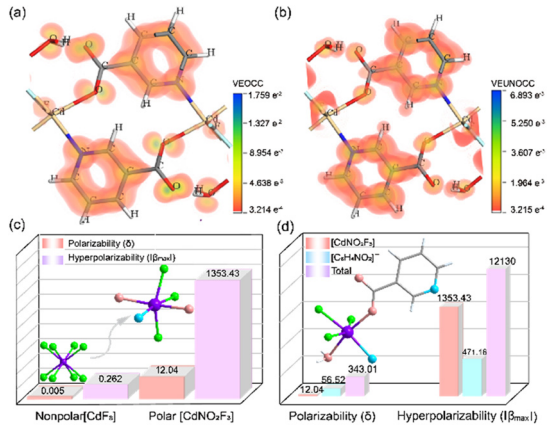

Fig. 5 SHG-weighted densities of the occupied (a) and unoccupied (b) states of $CdF(C_6H_4NO_2)(H_2O)$ in the virtual electron process. (c) Hyperpolarizability and polarization anisotropy calculations for the non-polar octahedron $[CdF_8]$ and the polar octahedron $[CdNO_2F_3]$. (d) Theoretical calculation of anisotropy and hyperpolarizability contributions of $CdF(C_6H_4NO_2)(H_2O)$, $[CdNO_2F_3]$ and $(C_6H_4NO_2)^-$.

(VH) processes are mainly from C-2p, N-2p, O-2p, and F-2p orbitals, while the unoccupied states are primarily from C-2p, N-2p, and Cd-4d orbitals. These findings confirm that the SHG density arises from the synergistic contributions of the $(C_6H_4NO_2)^-$ unit, F, and Cd atoms.

It is well known that anisotropy and hyperpolarizability are key parameters affecting second harmonic generation (SHG) and birefringence, respectively. We calculated these properties for $[CdF_8]$, $[CdNO_2F_3]$, $CdF(C_6H_4NO_2)(H_2O)$, and $(C_6H_4NO_2)$ using the LanL2DZ basis set in Gaussian[49] (Fig. 5c and d). For CdF_2, $[CdF_8]$ shows near-zero hyperpolarizability and anisotropy, consistent with its poor birefringence and lack of SHG. In contrast, $[CdNO_2F_3]$ in $CdF(C_6H_4NO_2)(H_2O)$ exhibits hyperpolarizability and anisotropy values over 2000 and 5000 times higher than those of $[CdF_8]$, highlighting its crucial role in enhancing optical properties (Fig. 5c). Fig. 5d shows that $(C_6H_4NO_2)^-$ significantly contributes to birefringence, while the highly polarized $[CdNO_2F_3]$ units drive strong SHG. Taken together, it is confirmed that the unique "Warren truss structure" formed by the π-conjugated organic ring $(C_6H_4NO_2)^-$ leads to highly polarized and well-aligned $[CdNO_2F_3]$ octahedra and $(C_6H_4NO_2)^-$, which is the key factor leading to the strong SHG and birefringence of $CdF(C_6H_4NO_2)(H_2O)$.

Conclusion

In summary, we have successfully synthesized $CdF(C_6H_4NO_2)(H_2O)$, a novel UV NLO material with a unique "Warren truss structure". Compared to CdF_2, which exhibits zero SHG effect and extremely low birefringence (0.00002@546 nm), $CdF(C_6H_4NO_2)(H_2O)$ demonstrates remarkable enhancements in both properties, achieving a large SHG response (3.2×KDP) and high birefringence (0.26@546 nm). These striking improvements are attributed to the introduction of the π-conjugated organic ring $(C_6H_4NO_2)^-$, which leads to the formation of a highly polarized and well aligned $[CdNO_2F_3]$ octahedra. Notably, this is the first UV fluoride material to simultaneously exhibit a large band gap (>4.2 eV), strong SHG effect (>3×KDP), and high birefringence (>0.2), making it a promising candidate for quantum optical technologies. Our study provides valuable insights into the design of non-centrosymmetric optoelectronic materials by constructing novel structures that activate high polarization and enhance optical properties.

Data availability

The data supporting this article have been included as part of the ESI.†

Conflicts of interest

The authors declare no competing financial interest.

Acknowledgements

This work is supported by the National Natural Science Foundation of China (22275052) and Department of Science and Technology of Hubei Province (2021CSA076).

References

1 Q. Xu, Y. Liu, Q. Wu, L. Hou, Y. Li, L. Li, Z. Lin, S. Zhao and J. Luo, A BBO-like trithiocyanate with significantly enhanced birefringence and second-harmonic generation, *Sci. China Mater.*, 2023, **66**, 3271–3277.
2 Y. Tang, K. Li, X. Zhang, J. Deng, G. Li and E. Brasselet, Harmonic spin–orbit angular momentum cascade in nonlinear optical crystals, *Nat. Photonics*, 2020, **14**, 658–662.
3 Y. Zhou, Z. Guo, H. Gu, Y. Li, Y. Song, S. Liu, M. Hong, S. Zhao and J. Luo, A solution-processable natural crystal with giant optical anisotropy for efficient manipulation of light polarization, *Nat. Photonics*, 2024, **18**, 922–927.
4 X. Lian, W. Yao, W. Liu, R. Tang and S. Guo, KNa_2ZrF_7: a mixed-metal fluoride exhibits phase-matchable second-harmonic-generation effect and high laser-induced damage threshold, *Inorg. Chem.*, 2020, **60**, 19–23.
5 G. Shi, Y. Wang, F. Zhang, B. Zhang, Z. Yang, X. Hou, S. Pan and K. R. Poeppelmeier, Finding the next deep-ultraviolet nonlinear optical material: $NH_4B_4O_6F$, *J. Am. Chem. Soc.*, 2017, **139**, 10645–10648.
6 X. Dong, L. Huang, C. Hu, H. Zeng, Z. Lin, X. Wang, K. M. Ok and G. Zou, $CsSbF_2SO_4$: an excellent ultraviolet nonlinear optical sulfate with a $KTiOPO_4$(KTP)–type structure, *Angew. Chem., Int. Ed.*, 2019, **131**, 6598–6604.
7 J. Zhou, H. Wu, H. Yu, S. Jiang, Z. Hu, J. Wang, Y. Wu and P. S. Halasyamani, $BaF_2TeF_2(OH)_2$: a UV nonlinear optical

fluorotellurite material designed by band-gap engineering, *J. Am. Chem. Soc.*, 2020, **142**, 4616–4620.

8 T. T. Tran, J. Young, J. M. Rondinelli and P. S. Halasyamani, Mixed-metal carbonate fluorides as deep-ultraviolet nonlinear optical materials, *J. Am. Chem. Soc.*, 2017, **139**, 1285–1295.

9 B. Wu, C. Hu, R. Tang, F. Mao, J. Feng and J. Mao, Fluoroborophosphates: a family of potential deep ultraviolet NLO materials, *Inorg. Chem. Front.*, 2019, **6**, 723–730.

10 Q. Ding, X. Zhang, Z. Lin, Z. Xiong, Y. Wang, X. Long, S. Zhao, M. Hong and J. Luo, Designing a deep-UV nonlinear optical monofluorophosphate, *Sci. China: Chem.*, 2022, **65**, 1710–1714.

11 Y. Sun, C. Lin, S. Fang, H. Tian, N. Ye and M. Luo, $K_2(BeS)O_4F_2$: a novel fluorosulfate with unprecedented 1D $[(BeO_3F)^-(SO_3F)]_\infty$ chains exhibiting large birefringence, *Inorg. Chem. Front.*, 2022, **9**, 6490–6497.

12 T. Wu, X. Jiang, C. Wu, Z. Lin, Z. Huang, M. G. Humphrey and C. Zhang, $Ce_3F_4(SO_4)_4$: cationic framework assembly for designing polar nonlinear optical material through fluorination degree modulation, *Inorg. Chem. Front.*, 2023, **10**, 5270–5277.

13 C. Wu, T. Wu, X. Jiang, Z. Wang, H. Sha, L. Lin, Z. Lin, Z. Huang, X. Long and M. G. Humphrey, Large second-harmonic response and giant birefringence of $CeF_2(SO_4)$ induced by highly polarizable polyhedra, *J. Am. Chem. Soc.*, 2021, **143**, 4138–4142.

14 J. Chen, C. L. Hu, X. H. Zhang, B. X. Li, B. P. Yang and J. G. Mao, $CsVO_2F(IO_3)$: an excellent SHG material featuring an unprecedented 3D $[VO_2F(IO_3)]^-$ anionic framework, *Angew. Chem., Int. Ed.*, 2020, **59**, 5381–5384.

15 J. Chen, C. L. Hu, F. F. Mao, J. H. Feng and J. G. Mao, A Facile Route to Nonlinear Optical Materials: Three–Site Aliovalent Substitution Involving One Cation and Two Anions, *Angew. Chem., Int. Ed.*, 2019, **58**, 2098–2102.

16 G. Zou, L. Huang, N. Ye, C. Lin, W. Cheng and H. Huang, $CsPbCO_3F$: A strong second-harmonic generation material derived from enhancement via p–π interaction, *J. Am. Chem. Soc.*, 2013, **135**, 18560–18566.

17 M. Liang, C. Hu, F. Kong and J. Mao, $BiFSeO_3$: an excellent SHG material designed by aliovalent substitution, *J. Am. Chem. Soc.*, 2016, **138**, 9433–9436.

18 Y. Hou, H. Wu, H. Yu, Z. Hu, J. Wang and Y. Wu, An Effective Strategy for Designing Nonlinear Optical Crystals by Combining the Structure–Directing Property of Oxyfluorides with Chemical Substitution, *Angew. Chem., Int. Ed.*, 2021, **60**, 25302–25306.

19 Y. Hu, C. Wu, X. Jiang, Z. Wang, Z. Huang, Z. Lin, X. Long, M. G. Humphrey and C. Zhang, Giant second-harmonic generation response and large band gap in the partially fluorinated mid-infrared oxide $RbTeMo_2O_8F$, *J. Am. Chem. Soc.*, 2021, **143**, 12455–12459.

20 J. Chen, C. Hu, Y. Lin, Y. Chen, Q. Chen and J. Mao, $K_3V_2O_3F_4(IO_3)_3$: a high-performance SHG crystal containing both five and six-coordinated V^{5+} cations, *Chem. Sci.*, 2022, **13**, 454–460.

21 H. Yu, M. L. Nisbet and K. R. Poeppelmeier, Assisting the effective design of polar iodates with early transition-metal oxide fluoride anions, *J. Am. Chem. Soc.*, 2018, **140**, 8868–8876.

22 Y. Hu, X. Jiang, C. Wu, Z. Huang, Z. Lin, M. G. Humphrey and C. Zhang, $A_2MoO_2F_3(IO_2F_2)$(A = Rb, Cs): Strong Nonlinear Optical Responses and Enlarged Band Gaps through Fluorine Incorporation, *Chem. Mater.*, 2021, **33**, 5700–5708.

23 P. Li, C. Hu, F. Kong and J. Mao, The first UV nonlinear optical selenite material: fluorination control in CaYF $(SeO_3)_2$ and Y_3F $(SeO_3)_4$, *Angew. Chem., Int. Ed.*, 2023, **62**, e202301420.

24 M. Yan, R. Tang, W. Yao, W. Liu and S. Guo, From $CaBaM_2F_{12}$ to $K_2BaM_2F_{12}$ (M = Zr, Hf): Heterovalent Cation-Substitution-Induced Symmetry Break and Nonlinear-Optical Activity, *Inorg. Chem.*, 2024, **63**, 10949–10953.

25 M. Yan, R. Tang, W.-D. Yao, W. Liu and S. Guo, Exploring a new short-wavelength nonlinear optical fluoride material featuring unprecedented polar cis-$[Zr_6F_{34}]^{10-}$ clusters, *Chem. Sci.*, 2024, **15**, 2883–2888.

26 (*a*) Y. Li, X. Zhang, Y. Zhou, W. Huang, Y. Song, H. Wang, M. Li, M. Hong, J. Luo and S. Zhao, An optically anisotropic crystal with large birefringence arising from cooperative π orbitals, *Angew. Chem.*, 2022, **134**, e202208811; (*b*) L. Wu, H. Fan, C. Lin and M. Luo, Compounds consisting of coplanar π-conjugated B_3O_6-typed structures: An emerging source of ultraviolet nonlinear optical materials, *Chin. J. Struct. Chem.*, 2023, **42**, 100019.

27 M. Xu, Q. Chen, B. Li, K. Du and J. Chen, π-Lone pair synergy in $(C_7H_4NO_4)(IO_3)$: Optimal balance among SHG, birefringence, and bandgap performance, *Chin. Chem. Lett.*, 2024, 110513.

28 H. Jia, D. Xu, Z. Li, M. Arif, Y. Jiang and X. Hou, $(C_3N_6H_7)BF_4{\cdot}H_2O$ and $(C_3N_6H_7)SO_3CH_3{\cdot}H_2O$ with large birefringence induced by coplanar π-conjugated $[C_3N_6H_7]^+$ groups, *Inorg. Chem. Front.*, 2024, **11**, 8331–8338.

29 C. Hu, C. Shen, H. Zhou, J. Han, Z. Yang, K. R. Poeppelmeier, F. Zhang and S. Pan, $(C_3N_2H_5)B_3O_3F_2(OH)_2$: Realizing Large Birefringence via a Synergistic Effect between Anion F/OH–Ratio Optimization and Cation Activation, *Small Struct.*, 2024, **5**, 2400296.

30 X. Meng, X. Zhang, Q. Liu, Z. Zhou, X. Jiang, Y. Wang, Z. Lin and M. Xia, Perfectly Encoding π–Conjugated Anions in the RE_5 $(C_3N_3O_3)(OH)_{12}$(RE = Y, Yb, Lu) Family with Strong Second Harmonic Generation Response and Balanced Birefringence, *Angew. Chem.*, 2023, **135**, e202214848.

31 J. Lu, X. Liu, M. Zhao, X. Deng, K. Shi, Q. Wu, L. Chen and L.-M. Wu, Discovery of NLO semiorganic $(C_5H_6ON)^+(H_2PO_4)^-$: dipole moment modulation and superior synergy in solar-blind UV region, *J. Am. Chem. Soc.*, 2021, **143**, 3647–3654.

32 M. Li, X. Zhang, Z. Xiong, Y. Li, Y. Zhou, X. Chen, Y. Song, M. Hong, J. Luo and S. Zhao, A Hybrid Antiperovskite with

Strong Linear and Second–Order Nonlinear Optical Responses, *Angew. Chem.*, 2022, **134**, e202211151Y.

33 Y. Li, W. Huang, Y. Zhou, X. Song, J. Zheng, H. Wang, Y. Song, M. Li, J. Luo and S. Zhao, A High–Performance Nonlinear Optical Crystal with a Building Block Containing Expanded π–Delocalization, *Angew. Chem., Int. Ed.*, 2023, **62**, e202215145.

34 T. B. Mohammadi, R. Alizadeh, A. Jalalian, S. Seyfi and V. Amani, Two new coordination polymers of Tl(I) & Hg(II), based on nicotinic acid ligand: synthesis, characterization, crystal structure determination & DFT calculation, *J. Iran. Chem. Soc.*, 2024, **21**, 2159–2172.

35 S. Landi Jr, I. R. Segundo, E. Freitas, M. Vasilevskiy, J. Carneiro and C. J. Tavares, Use and misuse of the Kubelka-Munk function to obtain the band gap energy from diffuse reflectance measurements, *Solid State Commun.*, 2022, **341**, 114573.

36 R. Tang, W. Xu, X. Lian, Y. Wei, Y. Lv, W. Liu and S. Guo, Na_2CeF_6: A Highly Laser Damage–Tolerant Double Perovskite Type Ce(IV) Fluoride Exhibiting Strong Second–Harmonic Generation Effect, *Small*, 2024, **20**, 2308348.

37 Q. Wu, H. Liu, X. Meng, L. Kang, L. Yang, Z. Lin, Z. Hu, C. Zhong, X. Chen and J. Qin, KBi_4F_{13}: A New Nonlinear Optical Material with a large damage threshold, *Chin. J. Inorg. Chem.*, 2015, **31**, 1875–1880.

38 Y. Huang, X. Meng, P. Gong, Z. Lin, X. Chen and J. Qin, A study on $K_2SbF_2Cl_3$ as a new mid-IR nonlinear optical material: new synthesis and excellent properties, *J. Mater. Chem. C*, 2015, **3**, 9588–9593.

39 S. K. Kurtz and T. T. Perry, A powder technique for the evaluation of nonlinear optical materials, *J. Appl. Phys.*, 1968, **39**, 3798–3813.

40 R. Tang, X. Lian, X. Li, L. Huai, W. Liu and S. Guo, From $CsKTaF_7$ to $CsNaTaF_7$: Alkali Metal Cations Regulation to Generate SHG Activity, *Chem. – Eur. J.*, 2022, **28**, e202201588.

41 L. Mateos, M. O. Ramírez, I. Carrasco, P. Molina, J. F. Galisteo-López, E. G. Víllora, C. de las Heras, K. Shimamura, C. Lopez and L. E. Bausá, $BaMgF_4$: An Ultra–Transparent Two–Dimensional Nonlinear Photonic Crystal with Strong $\chi^{(3)}$ Response in the UV Spectral Region, *Adv. Funct. Mater.*, 2014, **24**, 1509–1518.

42 J. G. Bergman, G. R. Crane and H. Guggenheim, Linear and nonlinear optical properties of ferroelectric $BaMgF_4$ and $BaZnF_4$, *J. Appl. Phys.*, 1975, **46**, 4645–4646.

43 J. G. Bergman, D. S. Chemla, R. Fourcade and G. Mascherpa, Linear and nonlinear optical properties of Na_2SbF_5, *J. Solid State Chem.*, 1978, **23**, 187–190.

44 M. J. Dodge, Refractive properties of magnesium fluoride, *Appl. Opt.*, 1984, **23**, 1980–1985.

45 Z. Guoqing, X. Jun, C. Xingda, Z. Heyu, W. Siting, X. Ke, D. Peizhen and G. Fuxi, Growth and spectrum of a novel birefringent α-BaB_2O_4 crystal, *J. Cryst. Growth*, 1998, **191**, 517–519.

46 G. Ghosh, Dispersion-equation coefficients for the refractive index and birefringence of calcite and quartz crystals, *Opt. Commun.*, 1999, **163**, 95–102.

47 Z. Chen, Y. Wang and Q. Liu, A hydrogen-bonded inorganic-organic network with noncentrosymmetric structure exhibiting second-order nonlinear optical response, *Inorg. Chem. Commun.*, 2018, **98**, 150–153.

48 D. A. Kleinman, Nonlinear dielectric polarization in optical media, *Phys. Rev.*, 1962, **126**, 1977.

49 S. Chiodo, N. Russo and E. Sicilia, LANL2DZ basis sets recontracted in the framework of density functional theory, *J. Chem. Phys.*, 2006, **125**, 104107.